Simplified equivalent soil profiles based on liquefaction performance for shallow-founded structures

M. Millen, C. Ferreira, A. Gerace & A. Viana da Fonseca
CONSTRUCT-GEO, Faculty of Engineering, University of Porto, Porto, Portugal

ABSTRACT: Earthquake-induced liquefaction is responsible for considerable structural damage. However, conventional liquefaction assessment focuses only on triggering. In this paper, the evaluation of liquefaction is refocused to consider the performance of buildings. A new hazard-independent liquefaction classification is proposed where the soil profile is defined as an equivalent 3-layered soil profile. The classification consists of only three features, highly influential to the performance of buildings: the depth of the non-liquefying crust, and the thickness and liquefaction resistance of the potentially liquefiable layer. The influence of these parameters is explored with reference to changes of the ground surface acceleration and foundation bearing capacity. A procedure to obtain the 3-layered soil profile from CPT data is developed and set of soil profile classes are developed for rapid loss assessment purposes. The procedure and classes are demonstrated on a case study site considering 100 CPT from Christchurch and a comparison is made regarding the computed LSN value for the equivalent and CPT profiles.

1 INTRODUCTION

A recent focus on the time of liquefaction during strong shaking as a key measure of the expected level of damage to a building on shallow foundations has highlighted the importance of classifying liquefaction resistance using a standard seismic hazard or independent of the seismic hazard. The hazard-independent classification of liquefaction resistance (e.g. the cyclic stress ratio to liquefaction in 15 uniform cycles) is a key step in the context of performance-based design and assessment and loss assessment frameworks, where a range of seismic hazard levels are considered. The ability to rapidly evaluate the time of triggering for different ground motions would allow the development of more robust estimates of liquefaction damage using pre- and post-liquefaction, ground intensity measures (Kramer et al., 2016). The quantification of liquefaction, in terms of the key parameters that influence the performance of the building, should also reduce uncertainty when considering the influence of liquefaction on building performance. Along with the liquefaction resistance capacity, the two most important parameters identified in recent literature are the thickness of the non-liquefying crust and the height of the liquefied (or liquefiable) layer. These two parameters are shown to influence building settlement (e.g. Liu and Dobry, 1997; Shahir and Pak, 2010; Karamitros et al., 2013; Bertalot and Brennan, 2015; Lu, 2017), the characteristics and intensity of ground surface shaking (Bouckovalas et al., 2017), the manifestation of liquefaction at the surface (Ishihara, 1985; Ishihara et al., 1990) and the soil stiffness or foundation impedance (Karatzia et al., 2017).

While liquefaction classification in terms of triggering is useful for mapping, the hazard-independent classification does not preclude these assessments, since triggering maps can readily be obtained by combining the maps of seismic hazard and liquefaction resistance. This has the distinct advantage of being independent of regularly updated seismic hazard maps. Furthermore,

liquefaction triggering assessments that use different assumptions can provide considerably different results. Recent investigations of the performance of soil deposits in Christchurch during the 2011 earthquake by Cubrinovski et al. (2017) identified the role of pore water flow and seismic isolation as key differences between the CPT-based simplified triggering procedure from Boulanger and Idriss (2016) and nonlinear effective stress analyses. In turn, soil layers in terms of the normalised cone tip resistance and the information criterion were readily identified and consistent across both assessment procedures.

This paper proposes a simple three criteria, hazard-independent liquefaction classification system for performance and loss assessment of buildings on shallow foundations, using the height and depth to the critical liquefiable layer, as well as the average cyclic resistance of the liquefiable layer for 15 cycles of uniform load. The influence of these properties on ground surface shaking and bearing capacity are explored. The classification system is implemented as an algorithm and used to identify classification difficulties (e.g. in highly stratified soil). A set of criteria for classification of soil profiles for regional scale loss assessment are also presented and demonstrated on a case study site in Christchurch.

The main advantages of this approach are:

- Can be determined from CPT, DMT, SPT or borehole data
- Captures the soil profile performance across the full hazard range using just three values
- Information is directly related to building performance
- Intuitive, physically represented, easy-to-communicate parameters are used
- Can provide a definition of the profile without knowing the seismic hazard at the site

2 INFLUENCE OF PARAMETERS ON THE DEFINITION OF AN EQUIVALENT SOIL PROFILE

2.1 *Bearing capacity*

The bearing capacity of a foundation on a soil deposit in its liquefied state (degraded bearing capacity) is a key indicator of expected settlement and tilt (e.g. Karamitros et al., 2013; Bray and Macedo, 2017; Bullock et al., 2018). According to Karamitros et al. (2013) and Bray and Macedo (2017), the degraded bearing capacity can be computed according to Meyerhof and Hanna (1978), for a strong soil crust underlain by a weak soil layer. The degraded bearing capacity depends on the shear strength of the crust and the residual shear strength of the liquefied sand (Karamitros et al., 2013), at least for cases where the stress bulb of the foundation does not reach deeper more resistant and non-liquefiable soils.

To demonstrate the importance of the crust height, Figure 2 shows a series of calculations performed using Meyerhof and Hanna (1978) for different crust heights (H_{crust}), different crust undrained or total stress resistances – "cohesive" strengths (c_{crust}), different liquefied/degraded layer angle of shearing resistance – "equivalent" angle (ϕ_{deg}) and different foundation widths (B_f).

What is apparent is that for a strong crust and weak liquefiable layer strength, the thickness of the crust has a great influence on the degradation of the bearing capacity ($q_{ult,deg}/q_{ult,i}$). The influence of the crust becomes less important with increased strength of the liquefiable layer with respect to the crust. Also shown in Figure 2 are the lines corresponding to 2.5 times the foundation width. This is approximately equal to the point where the thickness of the crust no longer has an influence on the bearing capacity. The influence is less than this limit for wide foundations, if the liquefied soil is modelled with an equivalent friction angle, since the strength of the layer increases with depth, whereas assuming an equivalent cohesive strength (undrained or other derived in total stresses) would mean constant strength with depth. While the liquefied shear strength is a key parameter in the estimation of bearing capacity, it could also be expected to be highly correlated to the liquefaction resistance, as increased density typically results in increased liquefaction resistance and increased dilative behaviour.

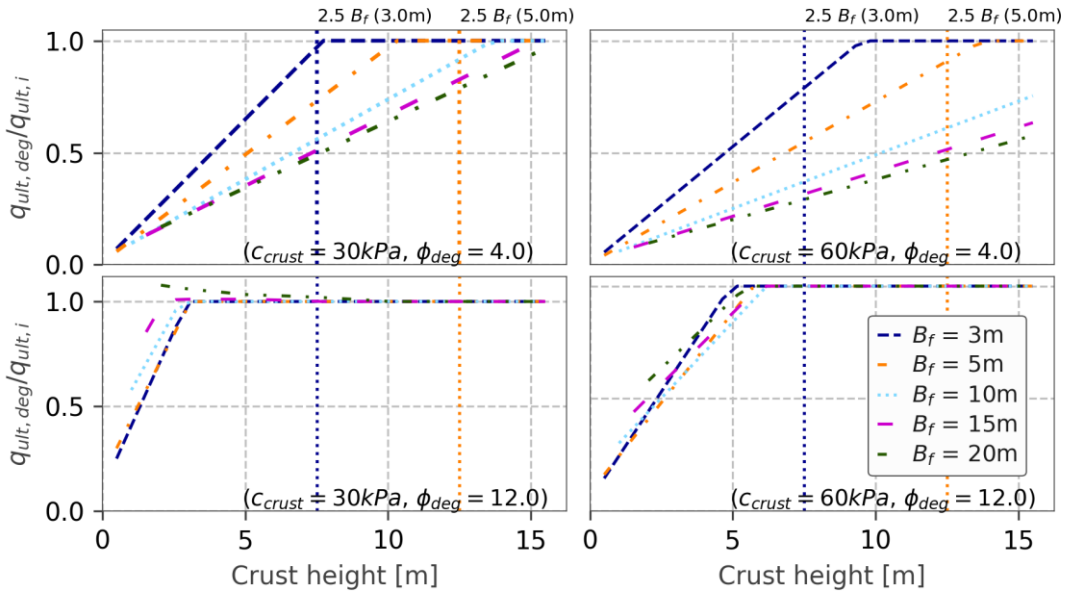

Figure 1. Influence of crust properties on bearing capacity

2.2 *Surface shaking*

Bouckovalas et al. (2017) proposed the Spectral Envelope Method, for approximating ground surface response spectra for a liquefied deposit where the liquefied and non-liquefied deposits are analysed with equivalent linear analyses and the envelope of the response spectrum from the pre and post liquefaction segments of the ground motion is considered the total surface response spectrum. This simple procedure provides unique insights into how the thickness of the crust, liquefiable layer and post-liquefaction stiffness influence the surface ground motion. While the liquefied shear stiffness is an influential parameter for estimation of the modification to the surface motion, it could also be highly correlated to the liquefaction resistance, since soil density is correlated with both liquefaction resistance and shear stiffness. Viana da Fonseca et al. (2018) reported the results of a series of linear analyses performed using the python package Pysra (Kottke, 2018) where the crust height, liquefiable layer height and ratio of shear stiffness between the liquefied and non-liquefied layers were varied (Figure 2). It is demonstrated that at low periods (high frequency) there is a strong reduction in the amplitude of shaking. For longer periods, this reduction switches to become an amplification, and eventually tends to no change in amplitude. The extent of periods that are amplified and de-amplified, as well as the magnitude of the amplification is clearly a function of the height of the crust, height of the liquefiable layer and the stiffness of the liquefiable layer. With a general shift to longer periods and for increasing crust and liquefied layer thickness, as well as decrease in liquefied layer stiffness.

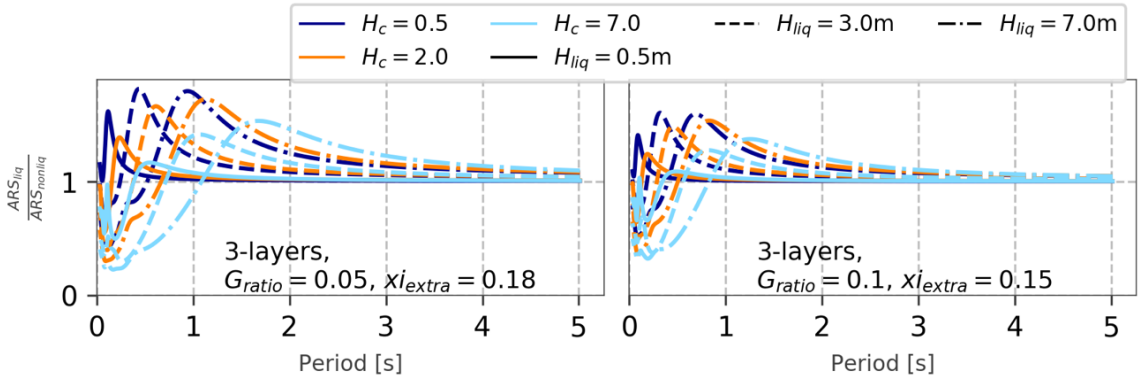

Figure 2. Influence of crust and liquefiable layer height on surface ground motion (adapted after Viana da Fonseca et al. 2018)

3 DEFINITION OF EQUIVALENT SOIL PROFILES

As discussed above, the influence of the layer thicknesses, the liquefied soil strength and the stiffness are continuous relationships, whereas regional scale loss modelling requires classification of the soil profile in discrete parts. The class limits for the cyclic resistance ratio at 15 cycles (Figure 3a), were set to provide a reasonable split between the different classes based on previously investigated CPT data presented in Boulanger and Idriss (2016). The limits are therefore arbitrary, but provide an intuitive tool for discussion of the performance of buildings as well as the time of liquefaction and post-liquefaction stiffness and strength.

The limits for delineating the depth and height of the liquefiable layer were proposed for the performance of idealised upper and lower limits of low-rise buildings (less than six storeys) on shallow foundations on flat ground. While some aspects of the performance are independent of the building height, very tall buildings or buildings on piled foundations may have less dispersion in performance if different criteria are chosen.

The minimum capacity of a soil deposit with a fully liquefied (zero liquefied strength) is approximately equal to two times the crust thickness times the equivalent cohesive strength of the crust. Therefore, a 2m thick 50kPa cohesive strength could sustain a minimum load of a 4m foundation with 50kPa load, and a 7m crust could sustain 10m foundation of 70kPa. Thus, the majority of buildings would have bearing capacity factors of safety less than one for the shallow liquefaction class and greater than one for the deep liquefaction class. The 2m crust and 3m liquefiable layer also corresponds to a change from de-amplification to amplification of surface spectral acceleration for periods greater than 0.25s, which represents approximately the maximum first mode period for a low-rise building if the infills remain intact. Whereas the 7m crust and 7m liquefiable layer corresponds to the change at 1s, which is approximately the upper limit for the first mode period for low-rise buildings with damaged infills and limited ductility. Therefore, if the infills remain intact, then liquefaction would generally decrease the shaking demand on the building for even the shallow thin liquefaction classes, however, if the infill is damaged then significant amplification could be expected unless the liquefaction is large. Obviously, because the relationships are continuous, each class is not homogenous and no major change in behaviour should be expected for a slight change in depth that would result in a change in soil class. The parameter definitions lead to 22 different equivalent soil profile (ESP) types (Figure 3b).

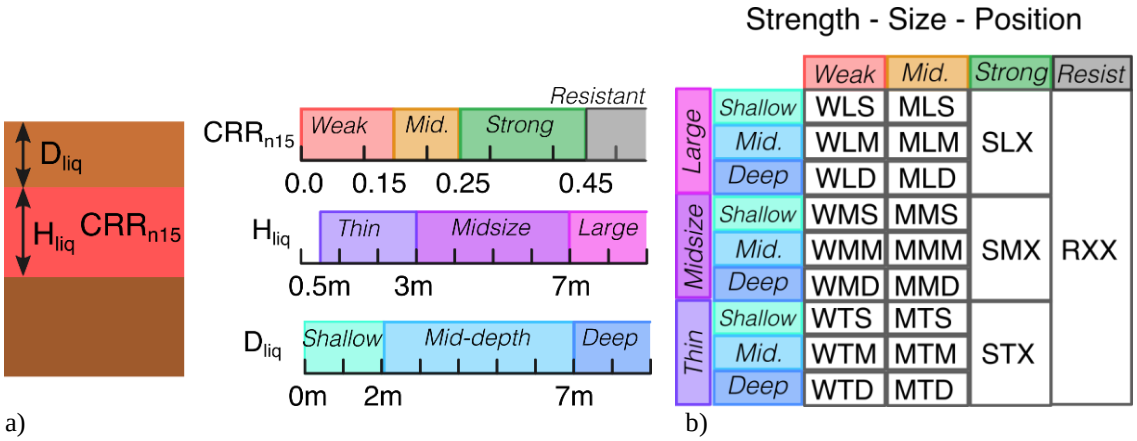

Figure 3. Equivalent soil profile classification: a) range definition; b) classes

4 PROCEDURE TO DEFINE ESP FROM CPT

The classification of a soil profile can be performed through cyclic element testing in the laboratory to identify key layers, but to allow efficient classification, it is more convenient and reliable to use continuous field data, namely through CPTu results. The procedure can be semi-automated by computing the CRR for a magnitude 7.5 earthquake using a simplified triggering procedure (e.g. Boulanger and Idriss, 2014), and fitting a three-layered profile to the CRR values. The procedure proposed here consists of computing every possible three-layered profile so as to minimise

the difference between the CRR values of the computed and the equivalent three-layered profiles, as schematically illustrated in Figure 4. The calculation of the error is sensitive to the value set to be the non-liquefying limit of CRR and the maximum depth of the profile. The non-liquefying limit was set to CRR=0.6, as this is a common limit used in simplified procedures (e.g. Youd et al., 2001; Boulanger and Idriss, 2014). Using a higher value means that soil layers with high CRR would generate some error during fitting (Gerace, 2018). The maximum depth was taken as 20 metres, since surficial consequences of liquefaction below such depths are negligible (Maurer et al., 2015). The increment of depths and CRR should be set small enough that they are not influential on the final results. The depth increment was set to 0.1m and the CRR increments were determined by setting the equivalent cone tip resistance for clean sand to range from 0 to 175 kPa in increments of 5kPa to give a CRR range from 0.061 to 0.6.

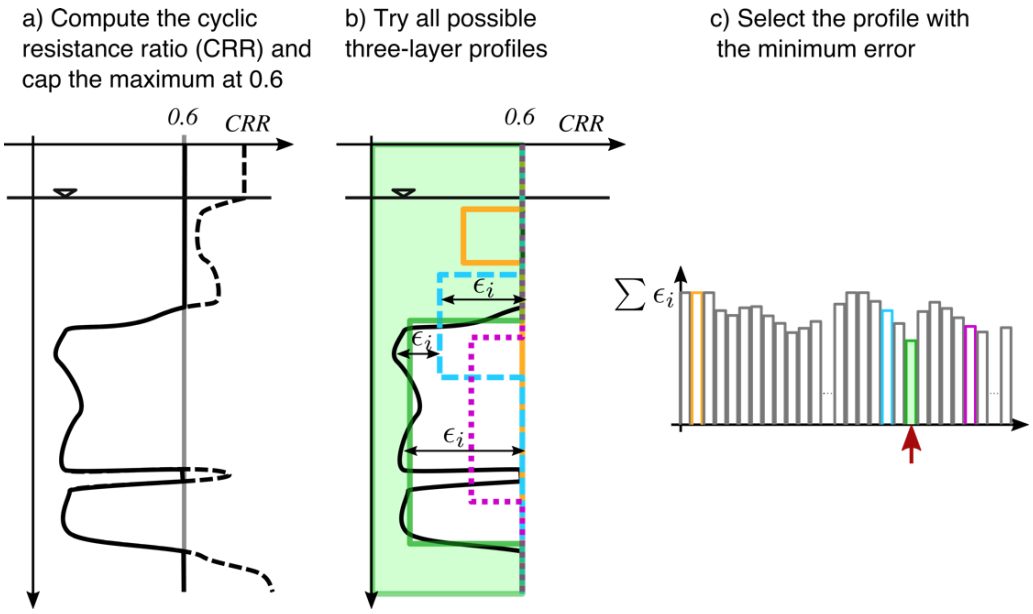

Figure 4. Procedure to implement the CRR-fitted method

The implemented algorithm (Figure 4) minimised the normalised difference $\tilde{\delta}$ (Equation 1), where CRR_{calc} and CRR_{fitted} are the calculated and fitted CRR values, ΔH is the depth increment of the calculated values, $CRR_{non-liq}$ is the non-liquefiable limit and H_{total} is the total height of the profile, capped at the maximum value of 20m.

$$\tilde{\delta} = \frac{\sum (CRR_{calc,i} - CRR_{fitted,i}) \cdot \Delta H}{CRR_{non-liq} \cdot H_{total}} \tag{1}$$

5 CASE STUDY RESULTS

In the 2010-2011 Canterbury Earthquake Sequence, severe and widespread liquefaction occurred over nearly half of the urban area of Christchurch (Cubrinovski et al., 2011). The liquefaction manifestation ranged from low or moderate to severe across various suburbs, and often was non-uniform even within a given suburb. Particularly severe liquefaction occurred in the eastern suburbs of Christchurch along the Avon River where lateral spreading also occurred (Cubrinovski and Robinson, 2016). Subsequently, extensive damage inspections and field investigations were carried out, especially where liquefaction occurred, providing a vast database of CPTu results. Further research studies have also been performed including in-depth analysis of particular aspects of soil liquefaction and its effects on buildings and infrastructure (Rhodes, 2017).

One of the sites in Christchurch where liquefaction phenomena occurred was around Sullivan Park, along the Avon River. At this site, more than 500 CPTu tests were performed and the results are available (via NZGD: www.nzgd.org.nz), from which 100 CPTu results have been randomly

selected. The procedure developed for ESP has been applied to these results, in order to assess the applicability of the classification algorithm. An example of the algorithm output for a single soil profile from Christchurch is provided in Figure 5, where the liquefiable layer was defined from 1.9m to 10.7m, ignoring the semi resistant soil at 4-6m. The LSN at different levels of PGA is compared in Figure 6a.

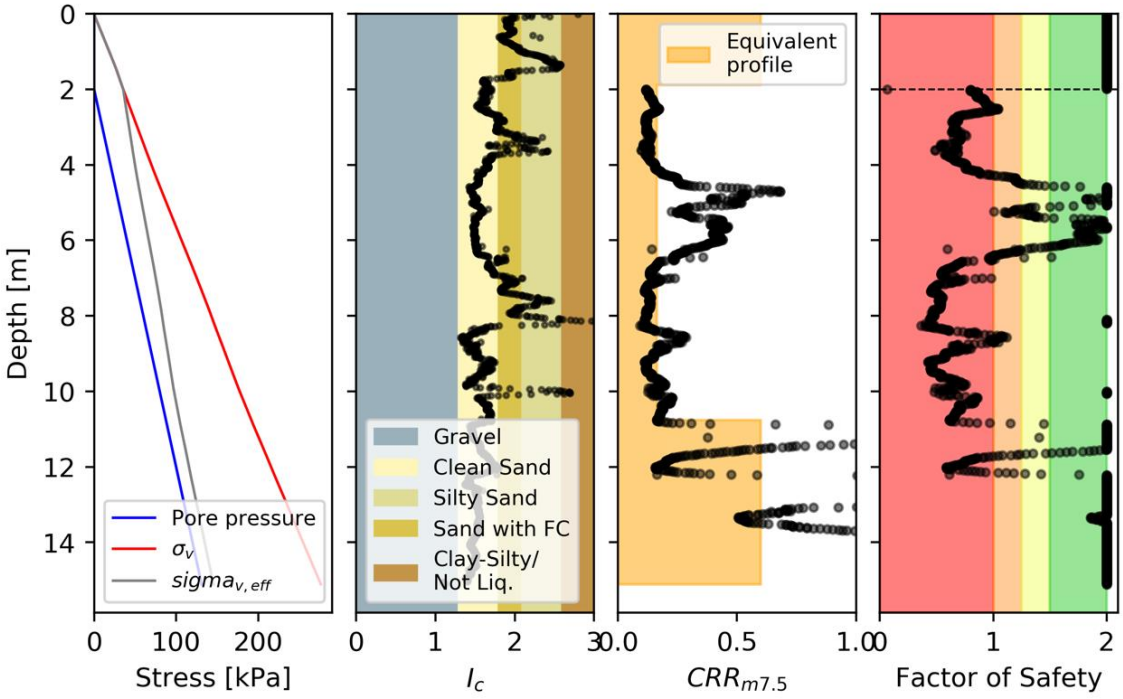

Figure 5. Case study single profile classified

The LSN for the ESP increases more rapidly than the CPT record since the soil resistance is considered more uniform. In this case the LSN values at very large PGA values are identical, however, the ESP profile has plateaued at 0.4g, whereas the more resistant layers (4-6m) in the CPT record would only reach maximum strain at PGA values above 0.6g. However, the LSN calculation assumes each 0.1m of the CPT record is independent, while pore water flow may result in much earlier liquefaction of the more resistant layers. It can been seen that the general trend is consistent between the two profiles and demonstrates that the reclassification of the soil profile into just three parameters still provides the general behaviour of the profile across the full hazard range.

The distribution of the soil profile classification in this site is provided in Figure 6b, from the analysis of 100 CPTu. This leads to the following breakdown on equivalent profile types: 34% of weak soil profiles, 65% of mid-strength, predominantly shallow, profiles and only 2% of strong soil profiles.

The statistical breakdown of Equivalent Soil Profiles (ESP) in a region can be used to inform macro liquefaction maps as in region-level estimation (microzonation), enabling susceptibility to be connected to vulnerability of buildings and critical infrastructures. At the region-level, a distribution of ESPs could be used to reflect the variability of the soil across a large area.

Recognizing that this methodology has some limitations, particularly using just three layers, limits the ability to investigate the influence of pore waterflow and effects such as lensing.

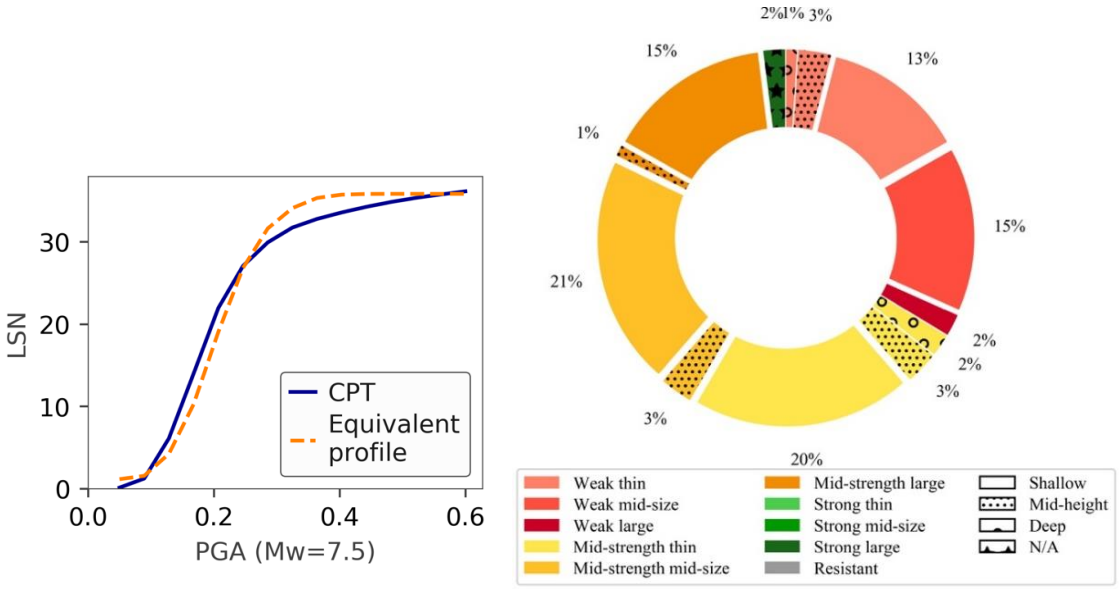

a) b)

Figure 6. Equivalent soil profile results: a) comparison of LSN vs PGA for the case study CPT; b) Christchurch equivalent soil profile distribution

6 CONCLUSIONS

This paper focused on introducing a new methodology for obtaining a simplified equivalent three-layered soil profile based on the liquefaction assessment of CPT data. The equivalent soil profile (ESP) is defined as a soil profile classification tool for the purpose of quantifying the seismic response of shallow-founded buildings on liquefiable soils. This methodology uses three governing parameters: the depth of the crust (D_{liq}), the thickness of the liquefied layer (H_{liq}) and its liquefaction resistance (CRR_{n15}). Typical ranges of values for each of these variables have been defined, from which 22 different soil profile classes were derived.

The calibration of the methodology was based on the analysis of 100 CPT tests at a site in Christchurch, in which a majority of mid-strength shallow profiles were classified. The comparison between the generated equivalent soil profiles and the respective LSN classification was established to demonstrate the applicability of this new simplified approach to the assessment of severity of liquefaction-induced damages. The use of this ESP classification for bearing capacity analysis in liquefied soils has the advantage of being capable of reproducing the response of the soil profile across the full hazard range using just three intuitive parameters, as the parameters are directly related to the performance of shallow-founded buildings.

ACKNOWLEDGEMENTS

This paper was produced as part of LIQUEFACT project (“Assessment and mitigation of liquefaction potential across Europe: a holistic approach to protect structures/infrastructures for improved resilience to earthquake-induced liquefaction disasters”) received funding from the European Union’s Horizon 2020 research and innovation programme under grant agreement No GAP-700748.

This work was also financially supported by: UID/ECI/04708/2019- CONSTRUCT - Instituto de I&D em Estruturas e Construções funded by national funds through the FCT/MCTES (PIDDAC). The second author acknowledges the support of the Portuguese Foundation for Science and Technology (FCT) through grant SFRH/BPD/120470/2016.

REFERENCES

Bertalot, D. & Brennan, A. J. 2015. Influence of initial stress distribution on liquefaction-induced settlement of shallow foundations. *Géotechnique*, 65(5): 418–428.

Bouckovalas, G. D., Tsiapas, Y. Z., Zontanou, V. A. & Kalogeraki, C. G. 2017. Equivalent Linear Computation of Response Spectra for Liquefiable Sites: The Spectral Envelope Method. *Journal of Geotechnical and Geoenvironmental Engineering 143*(4), 04016115–12.

Boulanger, R. W. & Idriss, I. M. 2016. CPT-Based Liquefaction Triggering Procedure. *Journal of Geotechnical and Geoenvironmental Engineering* 142(2), 04015065–11.

Boulanger, R.W. & Idriss, I.M. 2014. CPT and SPT based liquefaction triggering procedures. *Report No. UCD/CGM-14/01. Center for Geotechnical Modeling*, University of California, Davis. 134 pp.

Bray, J. D. & Macedo, J. 2017. 6th Ishihara lecture: Simplified procedure for estimating liquefaction-induced building settlement. *Soil Dynamics and Earthquake Engineering* 102: 215-231.

Bullock, Z., Dashti, S., Karimi, Z., Liel, A., Porter, K. & Franke, K. 2018. A physics-informed semi-empirical probabilistic model for the settlement of shallow-founded structures on liquefiable ground. *Géotechnique*, 1-14. doi:10.1680/jgeot.17.P.174.

Cubrinovski M. & Robinson K. 2016. Lateral spreading: Evidence and interpretation from the 2010–2011 Christchurch earthquakes, *Soil Dynamics and Earthquake Engineering*, 91: 187–201.

Cubrinovski, M., Bray, J., Taylor, M., Giorgini, S., Bradley, B., Wotherspoon, L. & Zupan, J. 2011. Soil Liquefaction Effects in the Central Business District during the February 2011 Christchurch Earthquake. *Seismological Research Letters*, 82: 893-904.

Cubrinovski, M., Rhodes, A. Ntritsos, N.& van Ballegooy, S. 2017. System response of liquefiable deposits. In *3rd Int. Conf. Performance-based Design in Earthquake Geotechnical Engineering*, 1–18.

Gerace, A. 2018. *Equivalent simplified soil profiles for liquefaction assessment*. MSc Thesis, Univ. Porto.

Ishihara, K. 1985. Stability of natural deposits during earthquakes, *Proceedings of the 11th International Conference on Soil Mechanics and Foundation Engineering*, 1: 321-376.

Ishihara, K., Yasuda, S. & Yoshida, Y. 1990. Liquefaction- induced flow failure of embankments and residual strength of silty sands, *Soils and Foundations*, 30(3): 69-80.

Karamitros, D. K., Bouckovalas, G. D. & Chaloulos, Y. K. 2013. Seismic settlements of shallow foundations on liquefiable soil with a clay crust. *Soil Dynamics and Earthquake Engineering*, 46(C): 64–76.

Karatzia, X. A., Mylonakis, G. & Bouckovalas, G. D. 2017. Equivalent-linear Dynamic Stiffness of Surface Footings on Liquefiable Soil. In *COMPDYN*: 1–15.

Kottke, A. & Bot, S. 2018. Pysra v0.2.1. *Pypi - Python package repository*.

Kramer, S.L., Sideras, S.S. & Greenfield, M.W. 2016. The timing of liquefaction and its utility in liquefaction hazard evaluation, *Soil Dynamics and Earthquake Engineering*, 91: 133-146.

Liu, L. & Dobry, R. 1997. Seismic Response of Shallow Foundation on Liquefiable Sand. *Journal of Geotechnical and Geoenvironmental Engineering* 123(6): 557–567.

Lu, C. W. 2017. A Simplified Calculation Method for Liquefaction- Induced Settlement of Shallow Foundation. *Journal of Earthquake Engineering* 21(8): 1385-1405.

Maurer, B.W., Green, R.A & Taylor, O. 2015. Moving towards an improved index for assessing liquefaction hazard: Lessons from historical data. *Soils and Foundations*, 55(4): 778-787.

Meyerhof, G. G. & Hanna, A. M. 1978. Ultimate bearing capacity of foundations on layered soils under inclined load. *Canadian Geotechnical Journal* 15(4): 565–572.

Rhodes, A. 2017. *Liquefaction evaluation in stratified soils*. PhD thesis, University of Canterbury, NZ.

Shahir, H. & Pak, A. 2010. Estimating liquefaction-induced settlement of shallow foundations by numerical approach. *Computers and Geotechnics* 37(3): 267–279.

Viana da Fonseca et al. 2018. Methodology for the liquefaction fragility analysis of critical structures and infrastructures: description and case studies, LIQUEFACT Proj. Deliverable D3.2, *Horizon 2020 European Union funding for Research & Innovation Project ID: 700748* (www.liquefat.eu).

Youd, T. L. et al. 2001. Liquefaction Resistance of Soils: Summary Report. *Journal of Geotechnical and Geoenvironmental Engineering*: 1–17.